Effects of Traveling Wave Ion Mobility Separation on Data Independent Acquisition in Proteomics Studies

Pavel V. Shliaha,[†] Nicholas J. Bond,[†,‡] Laurent Gatto, and Kathryn S. Lilley*

Cambridge Centre for Proteomics, Department of Biochemistry, University of Cambridge, 80 Tennis Court Road, CB2 1GA, United Kingdom

S *Supporting Information*

ABSTRACT: qTOF mass spectrometry and traveling wave ion mobility separation (TWIMS) hybrid instruments (q-TWIMS-TOF) have recently become commercially available. Ion mobility separation allows an additional dimension of precursor separation inside the instrument, without incurring an increase in instrument time. We comprehensively investigated the effects of TWIMS on data-independent acquisition on a Synapt G2 instrument. We observed that if fragmentation is performed post TWIMS, more accurate assignment of fragment ions to precursors is possible in data independent acquisition. This allows up to 60% higher proteome coverage and higher confidence of protein and peptide identifications. Moreover, the majority of peptides and proteins identified upon application of TWIMS span the lower intensity range of the proteome. It has also been demonstrated in several studies that employing IMS results in higher peak capacity of separation and consequently more accurate and precise quantitation of lower intensity precursor ions. We observe that employing TWIMS results in an attenuation of the detected ion current. We postulate that this effect is binary; sensitivity is reduced due to ion scattering during transfer into a high pressure "IMS zone", sensitivity is reduced due to the saturation of detector digitizer as a result of the IMS concentration effect. This latter effect limits the useful linear range of quantitation, compromising quantitation accuracy of high intensity peptides. We demonstrate that the signal loss from detector saturation and transmission loss can be deconvoluted by investigation of the peptide isotopic envelope. We discuss the origin and extent of signal loss and suggest methods to minimize these effects on q-TWIMS-TOF instrument in the light of different experimental designs and other IMS/MS platforms described previously.

KEYWORDS: traveling wave ion mobility separation, ion mobility separation, mass spectrometry, saturation, HDMS[E]
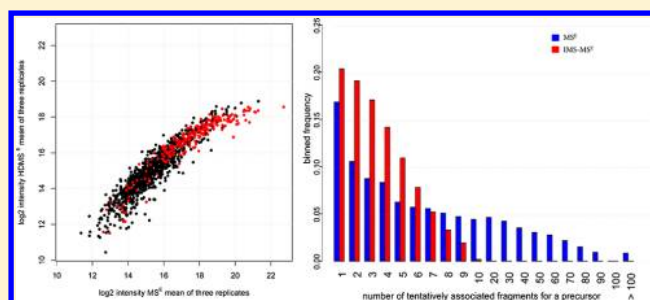
INTRODUCTION

Mass spectrometry has become the principal technique of proteomics in the recent years.[1] Proteins are typically digested to peptides, which are analyzed by liquid chromatography coupled to tandem mass spectrometry (LC−MS/MS).[2-4] Peptide identifications are then used to infer protein constituents in the original sample. While initial proteomics studies mostly focused on cataloguing proteins in the samples, more recent studies attempt to provide quantitative information on protein abundance.[1]

In the majority of quantitative proteomics methodologies, peptides are both identified and quantified.[2] Quantitation is typically performed either by using differential stable isotope labeling *in vivo*, such as SILAC,[3] or *in vitro*, such as isobaric tagging,[4] which allows simultaneous analysis of samples under comparison during LC−MS/MS. Alternatively, label-free approaches involve individual analysis of each sample with quantitative comparisons taking place *in silico*.[5] These approaches fall into two main categories: spectral counting, where the number of peptide ions identified in an experiment is used as a surrogate of protein abundance,[6] and area under the curve, where intensity of either intact peptides (MS1)[7] or their

fragments (MS2)[8] is measured. It has been demonstrated previously that the MS1 signal of a peptide is directly proportional to its loading on a column for 2.5−3 orders of magnitude both in simple and complex mixtures.[9−11]

Typically, peptide identification involves fragmentation, commonly using collision induced dissociation (CID), and matching of the resulting fragments *in silico*.[2] Information pertaining to the sequence of the peptide can also be inferred from the behaviour of the unfragmented entity, for example, mass to charge ratios (*m/z*), retention time, and ion mobility.[12−14] The most common fragment spectrum acquisition mode is data dependent acquisition (DDA). During a DDA experiment, fragmentation spectra are acquired by sequentially isolating and fragmenting peptide ions providing that certain criteria (set *a priori*) related to the precursors have been satisfied. The *m/z* of the precursor ion and corresponding fragment ions are then submitted to a search engine and matched against sequences within a database, working on the premise that the fragments observed derive exclusively from the

peptide isolated.[2] The limitations of this method include co-selection of several ions during the fragmentation process, semi-stochastic selection of ions for fragmentation, and under-sampling, all of which result in a lack of inter-run and inter-lab reproducibility,[15] a large number of single peptide protein identifications[16] and many unidentified proteins.[17] Moreover, as the quality of a spectrum is related to the amount of precursor ion fragmented, identifying a reasonable amount of peptides may require a substantial proportion of time spent in MS2 mode, which compromises the accuracy of all MS1 "area under the curve" quantitation methods[7] and thus instrument parameters promoting the maximum number of identifications may compromise the accuracy of quantification.

Several methods have been suggested that effectively combine DDA with area under the curve quantitation. One such approach, gas phase fractionation,[18] attempts to fragment different sets of peptides during repeated injections (necessary for accurate quantitation) of the same sample. This is done by specifying different mass ranges for selecting precursors for fragmentation during subsequent runs. This allows significantly deeper coverage of the proteome even with a low number of CID fragmentations per survey scan. Other researchers have suggested performing quantitation runs under optimal conditions and then targeting peptides that demonstrated differential abundance (MS1 intensity) in subsequent MS/MS runs by applying an inclusion list.[10]

Several research groups have attempted to circumvent the limitations of DDA by coselecting several ions for simultaneous fragmentation. For example, Masselon and co-workers used Fourier transform ion cyclotron resonance (FT-ICR), allowing selection and fragmentation of a combination of ions of any m/z using a SWIFT waveform.[19] This method is similar to DDA since ions are coselected for fragmentation based on their intensity.

Another approach to overcome DDA's limitations is to employ data independent acquisition (DIA) methods that do not attempt to isolate specific precursors. Instead, a group of precursors covering a mass window of specific size are cofragmented. Depending on the size of the mass selection window, instrument speed and sensitivity, a number of injections may be required to cover the entire mass range.[20,21,12,8,22] Fragment ions are expected to have the same elution and mobility profiles as their precursors, which can be used to pair fragments and precursors when a number of parent ions are cofragmented. Some DIA methods attempt to retrospectively pair fragments and their precursors prior to database searching, for example, parallel fragmentation approach,[23−25] MS[E,12] AIF,[22] and SWATH,[8] while others do not.[20,21]

Clemmer and co-workers used an in-house LC-IMS-MS platform to acquire precursors (MS1) and fragments (MS2) across the whole mass range. In their experimental design, the instrument cycles between a "low energy" scan, during which intact precursor masses are recorded (MS1 data) and a "high energy" scan, during which the cofragmentation of all precursors occurs by applying a collision energy ramp and the resultant fragment masses are recorded (MS2 data). The method was named the "parallel fragmentation approach" to emphasize that all precursors are recorded and fragmented. Since no ion selection is performed, many comeasurements can be made and accurate retention time and drift time profiles can be constructed for precursors and fragment ions.[7] Precursors and fragments are retrospectively paired based on the similarity

of their elution and mobility profiles. A similar method was later commercialized as MS[E,12] by the Waters Corporation. The primary difference of the MS[E] data acquisition workflow compared to the method developed by Clemmer and co-workers is that in MS[E] data can be analyzed by ProteinLynx Global SERVER (PLGS),[12] Waters Corporation proprietary software, which operates on a different premise than DDA search engines. During MS[E] data analysis in PLGS, fragments are initially associated with precursors by the similarity of their retention time profile. An iterative depletion process is then employed whereby a single protein is identified at a time and all of its associated peptides and their fragments are removed from the data before the depletion cycle continues. This protein-centric search results in high protein coverage. Initially, fragments were assigned to precursors within the PLGS workflow solely based on the similarity of retention time profiles.

More recently, Waters launched a new Synapt instrument series where TOF mass spectrometry is combined with TWIMS (traveling wave ion mobility separation). A TWIMS device allows separation based on ion mobility and subsequent measurement of all ions. Precursors and their corresponding fragments can then be matched based on the similarity of their mobility profiles.[26] When ion mobility separation is used in conjunction with the MS[E] workflow it is referred to as HDMS[E]. An additional benefit of IMS is increased accuracy of quantitation for lower abundance peptides and a higher dynamic range for peptide detection.[24,27,28] Valentine et al. noted that in complex samples upon application of IMS, peptides could be detected over 6 orders of magnitude in abundance, where only 5 orders of magnitude were possible without employing IMS. This increase is likely to result from enhanced deconvolution of low abundant peptide ions from contaminants and higher abundant peptides that occupy the same m/z and retention time space.[29] A similar effect of IMS has also been demonstrated recently by Geromanos et al. on Synapt G2 and G2-S platforms.[28]

The combination of TWIMS and qTOF into a single instrument results in a number of additional considerations in instrument design, however. First, the key to combining IMS and LC−MS/MS in a single instrument is the different time scales of LC, IMS and TOF separations, whereby IMS is much faster than LC, but much slower than TOF. A single IMS cycle is composed of a number of TOF separations. The IMS profile of an ion is the ion intensity distribution in these TOF separations. Since no ions can enter the "IMS zone" while IMS is in progress, ions entering IMS-MS hybrid instruments can either be discarded (which would lead to high losses of sensitivity) or trapped awaiting their turn to be subjected to IMS. Such a trapping device was introduced some years ago at the interface of the IMS drift tube by Hoaglund and co-workers.[31]

Second, the quadrupole and TOF require to be operated at significantly lower pressures than TWIMS.[32] This creates a challenge of significantly different pressure zones in ion path.

In light of the instrument design considerations presented above, we have conducted a study to comprehensively evaluate the effect TWIMS has on the qualitative and quantitative nature of DIA in Synapt G2 configuration. Using low complexity 6 protein digest and high complexity (E. coli digest standard spiked with the six protein digest) samples, we have carried out extensive analysis in both MS[E] and HDMS[E] and have compared

the proteome coverage, signal intensity and linearity of response between the acquisition modes.

We find that where the application of TWIMS greatly increases coverage of the proteome, it also leads to some reduction in the linearity of response and sensitivity and hence impairs accuracy of quantitation in the higher end of the signal intensity range. We describe the reasons behind our observations and suggest ways to overcome their potential limitations.

■ MATERIALS AND METHODS

Sample Preparation

In this study, we have used a set of six proteins as spikes: bovine serum albumin (A3059), rabbit glycogen phosphorylase B (P6635), human carbonic anhydrase (C4396), horse cytochrome C (C2506), chicken lysozyme (L6876) and bovine beta casein (C6905) (Sigma, St Louis, MO). Preparation of the spikes was performed in LoBind tubes (Eppendorf, Stevenage, UK). For each of the proteins, a 5 mg/mL solution of lyophilized protein powder in water was prepared and further diluted to 10 pmol/μL. The 10 pmol/μL solutions were subjected to amino acid analysis[33] (PNAC, AAA Service, Dept. Biochemistry, University of Cambridge[27]) to determine the exact protein concentration, which deviated from the expected by no more than 25% for all of the six proteins. The protein solutions were further diluted to 5 pmol/μL in 100 mM triethylamine ammonium bicarbonate (TEAB) pH 8.5 (according to amino acid analysis data). Disulfide bonds were reduced by incubation of proteins with 5 mM dithiothreitol for one hour at 40 °C. Next, free thiols were alkylated by incubation in darkness for thirty minutes with 15 mM iodoacetamide at room temperature. Proteins were digested by incubation with sequencing grade modified trypsin (Promega Ltd., Southampton, UK) at 37 °C overnight. Trypsin was added twice at 1:40 (w/w) protein to trypsin ratio, first when digestion was initiated and again after two hours into the digest. Following digestion the six protein digests were mixed at equimolar amounts and diluted to 100 fmol/μL and 25 fmol/μL in 3% acetonitrile (ACN), 0.1% formic acid.

For the six protein mixture experiment, each sample to be loaded was prepared as a separate mixture of a final volume of 200 μL as specified in Table 1. To each, 10 μL of 200 fmol/μL enolase digest standard (Waters, Product Number: 186002325) was added to allow normalization during data processing.

For the spike experiment conducted in a complex background, 200 μg of an E. coli digest standard (two vials, Waters, Product Number: 186003196) was resuspended in 400 μL of 3% acetonitrile (ACN), 0.1% formic acid (FA). The E. coli digest standard concentration was estimated by absorbance at 280 nm using a Nanodrop 1000 to be 0.4 μg/μL, which was

close to theoretical of 0.5 μg/μL. Three solutions were mixed to produce a separate dilution for each spike loading as described in Table 2: 100 fmol/μL or 25 fmol/μL of equimolar protein digest, 3% ACN, 0.1% FA, 0.4 μg/μL E. coli digest standard.

LC−MS Configurations

The peptides were separated using a nanoAcquity UPLC system (Waters). The aqueous mobile phase A was 0.1% formic acid. The organic mobile phase B was acetonitrile with 0.1% formic acid. The samples were injected in 10 μL volume using a partial loop method, trapped on Symmetry C18 5 μm, 180 μM × 20 mm precolumn (Waters) and desalted at 10 μL/min flow for 6 min with 100% A. The separation was performed on T3 1.8 μM, 75 μm × 250 mm (Waters) at 300 nL/min flow rate, with 0−50% B, using a 45 min gradient for six protein mixture experiments and 7−35% B, using a 90 min gradient for complex sample experiments. After separation, the column was washed with 80% mobile phase B for 5 min and re-equilibrated with 3% mobile phase B for 15 min. The column temperature was maintained at 30 °C. 500 fmol/μL [Glu[1]]-fibrinopeptide B was infused at 500 nL/min as a reference compound.

Mass spectrometric analysis of eluting peptides was performed on Synapt G2 mass spectrometer (Waters, Manchester, UK), using settings suggested by manufacturer. The Synapt G2 was operated such that alternate low and high energy scans of equal duration of 0.4 s were conducted for six protein mixture experiments and 0.9 s for complex sample experiments. Smaller duration scans were used in the six protein experiment, since chromatographic peaks were sharper due to a steeper gradient. Lock spray was acquired once every 30 s for 1 s period. For fragmentation in MS[E] mode the collision energy was linearly ramped in the Trap region of the TriWave from 14 to 40 V across the duration of high energy scan (see above). For fragmentation in HDMS[E] mode, the collision energy was linearly ramped in the Transfer region of TriWave from 21 to 44 V across the duration of high energy scan (see above). Higher collision energies, as suggested by the manufacturer, were applied in HDMS[E] mode to counteract the slight leak of gas into the Transfer from the IMS region of the TriWave. This leak has a slight cooling effect on the ions, which requires increasing collision energy ramp in HDMS[E] to achieve similar fragmentation efficiency between modes (personal communication with Waters Corp.).

During IMS analysis, ions were accumulated in the "Main body" of Trap region for 14.25 ms and then released into the "Transport part" of the Trap which continuously ran 6 V waves at 311 m/sec velocity. 450 μs mobility delay was applied before starting IMS. 40 V waves were applied in IMS part of TriWave at 650 m/s. 4 V waves were applied in transfer region of the instrument at the velocity of 190 m/sec.

Data Analysis

Data analysis was performed in PLGS version 2.5.2. Data were lock mass corrected post acquisition. Noise reduction thresholds for low energy scan ion, high energy scan ion and peptide intensity combined across charge states and isotopes were fixed at 150, 10, and 750 counts, respectively ("processing parameters" as suggested by manufacturer). During database searches, the protein false discovery rate was set at 4%. A peptide was required to have at least a single assigned fragment and protein was required to have at least one assigned peptide and three assigned fragments for identification.

Table 1. Dilution Series for Six Protein Mixture Experiment

sample loading (fmol/ injection)	concentration (fmol/μL)	total amount 200 μL (fmole)	volume of 100 fmol/μL equimolar protein digest (μL)	volume of 3% ACN, 0.1% FA	volume of 200 fmol/ μL enolase solution
20	2	400	4	186	10
50	5	1000	10	180	10
100	10	2000	20	170	10
200	20	4000	40	150	10
500	50	10000	100	90	10

Table 2. Dilution Series for Complex Sample Experiment

loading (fmol/injection)	concentration (fmol/μL)	total amount 150 μL (fmole)	volume of 25 fmol/μL equimolar protein digest (μL)	volume of 100 fmol/μL equimolar protein digest (μL)	volume of 0.4 ug/μL E. coli standard (μL)	volume of 3% ACN, 0.1% FA (μL)
25	2.5	375	15	–	40	95
50	5	750	30	–	40	80
75	7.5	1125	45	–	40	65
100	10	1500	–	15	40	95
150	15	2250	–	22.5	40	87.5
250	25	3750	–	37.5	40	72.5
500	50	7500	–	75	40	35

■ RESULTS

We have conducted a study to comprehensively evaluate the effect TWIMS has on the qualitative and quantitative nature of DIA. In order to do this, low complexity (6 protein digest) and high complexity (E. coli digest standard spiked with six proteins) samples were analyzed in both MS^E and HDMS^E (IMS-MS^E) acquisition modes. While the 6 protein digest analysis was designed to represent LC–MS of a simple protein mixture enriched in high abundance constituents (e.g., plasma samples, IP-MS experiments), the complex sample was designed to represent shotgun analysis of a whole cell lysate. A comparison of proteome coverage, signal intensity and linearity of response was made between modes. For thorough examination of the data, comparisons were performed at the ion, peptide and protein levels.

HDMS^E Produces a Higher Number of Protein Identifications

The perceived advantage of DIA over DDA, is that all precursor ions and their fragment ions are measured assuming they are sufficiently abundant to be detected above noise, that is, above the limit of detection (LOD). The main limitation of the technique is the inability to unambiguously assign all fragments to precursors. Workflows specifically designed for DIA analysis will attempt to deconvolute a fragment's origin prior to database searching (parallel fragmentation,[23−25] MS^E,[13] AIF,[21] SWATH[5]). In PLGS, initially all low molecular weight precursors and fragments that are not expected to have high sequence specificity are filtered out. Fragments are tentatively associated with precursors based on the similarity of their retention time (and if available, their mobility profiles) and the premise that a fragment should not have higher intensity than a precursor. All fragments that have an elution profile apex within plus or minus one-tenth of the chromatographic peak width of a precursor and an IM profile apex within plus or minus 1 drift bin of a precursor, are tentatively associated with that precursor. Assignment of fragments to precursors based solely on similarity of retention time profiles is quite crude and a typical fragment is often associated with a number of precursors. Thus DIA methods should theoretically benefit from incorporating IMS in to the workflow.[6]

To demonstrate this effect, we first analyzed the E. coli digest standard in DIA modes with and without IMS separation. Different amounts (0.0625, 0.125, 0.25, 0.5, 0.75, and 1 μg) of sample were analyzed to assess the sensitivity of DIA with and without IMS with respect to sample loading. The numbers of peptide and protein identification are presented in Table 3. We found that while MS^E produced a more or less consistent number of identifications in the range of 0.25−1 μg of sample analyzed, HDMS^E consistently produced significantly more identifications with increased loading.

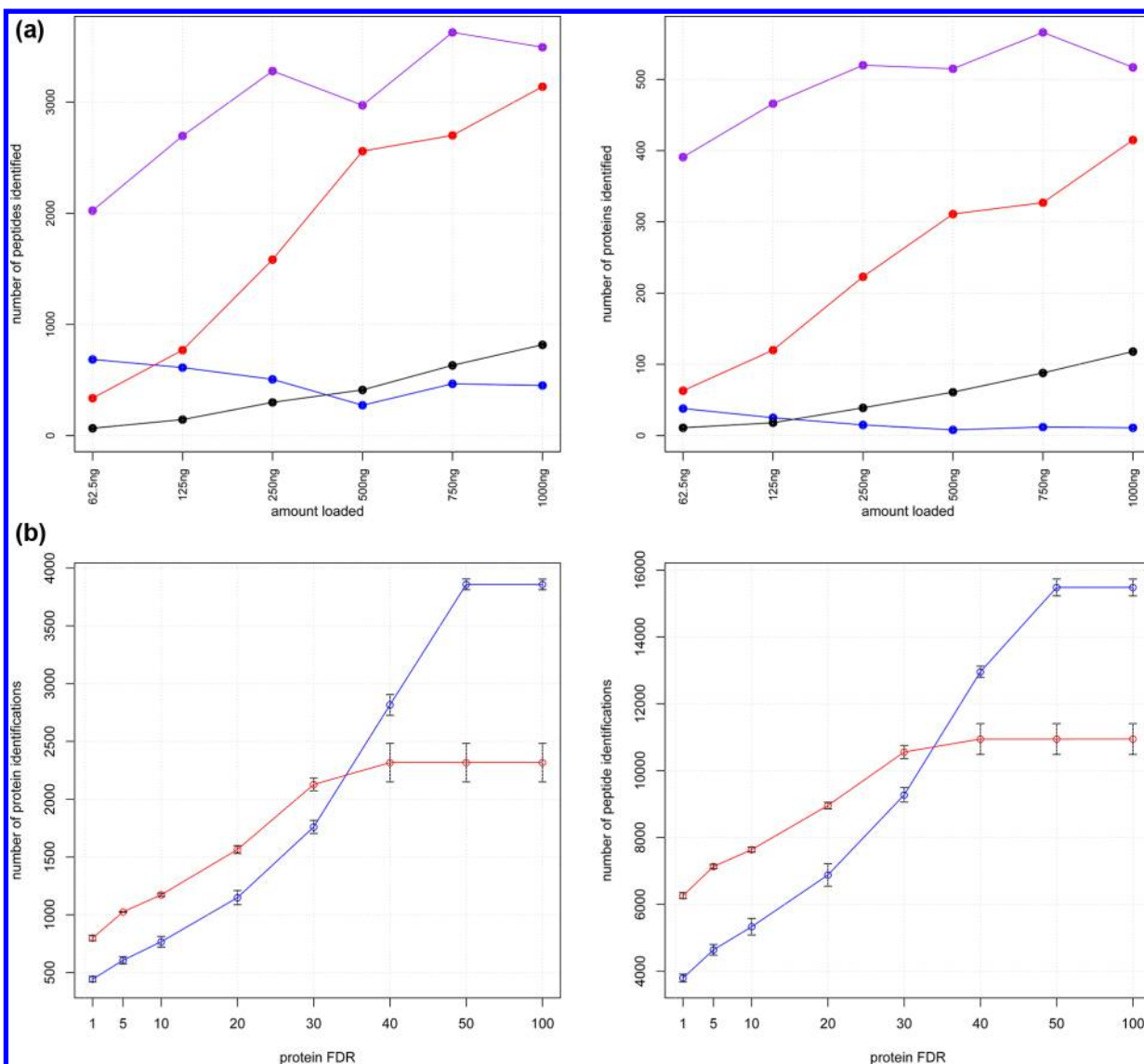**Table 3. Number of Protein and Peptide Identifications at Different Amounts of E. coli Digest Standard Analyzed[a]**

loading	MS^E protein identifications	HDMS^E protein identifications	MS^E peptide identifications	HDMS^E peptide identifications
0.0625	444 ± 15	454 ± 10	2749 ± 6	2379 ± 53
0.125	510 ± 18	601 ± 7	3416 ± 58	3559 ± 26
0.25	561 ± 19	758 ± 27	4017 ± 64	5072 ± 184
0.5	600 ± 29	840 ± 76	4394 ± 164	5816 ± 664
0.75	598 ± 31	933 ± 12	4509 ± 243	6683 ± 259
1	553 ± 23	957 ± 38	4342 ± 133	6982 ± 78

[a]Numbers shown are averages of three replicates plus minus standard deviation.

It is noteworthy that analysis of 1 μg of E. coli digest standard in HDMS^E produced on average an increase of 58% peptide and 60% protein identifications over the analysis of E. coli digest standard in MS^E at the most optimal loading (0.5 μg).

When analyzing the overlap between identifications of peptides and proteins made with and without IMS, we found that with increased loading (Figure 1a) the number of identifications at 4% protein FDR unique to MS^E decreases and the number of identifications unique to HDMS^E and common to MS^E and HDMS^E increases. We also tested the effect that the protein FDR specified during database searching has on the number of identified peptides and proteins in both modes (using acquisitions of 1 μg of E. coli digest standard). Figure 1b demonstrates that at low FDR, more peptides and proteins are identified in HDMS^E. If a high FDR is accepted, however, HDMS^E provides less identifications, thus IMS of precursors before fragmentation allows deeper proteome coverage and reduces the number of false positives identifications at high FDR.

To explain this effect we compared the number of fragments that could be tentatively associated with a precursor prior to database searching, based on similarity of their chromatographic elution and ion mobility profiles in HDMS^E, and elution profile only in MS^E. We found 54600 precursors and 1.24×10^6 fragment EMRTs (Exact Mass Retention Time Pair) in MS^E and 35500 precursors and 2.21×10^6 fragment EMRTs in HDMS^E passed our LOD threshold (specified as "processing parameters"). Figure 2 demonstrates the distribution of binned frequency for the number of tentatively associated fragments for MS^E and HDMS^E precursors and conversely tentatively associated precursors for MS^E and HDMS^E fragments. Clearly HDMS^E is much more selective in fragment assignment, having on average 226 tentative fragments per precursor compared to MS^E with 851 tentative fragments per precursor. An average fragment was tentatively associated with 37.5 precursors in MS^E and 3.62 precursors in HDMS^E.
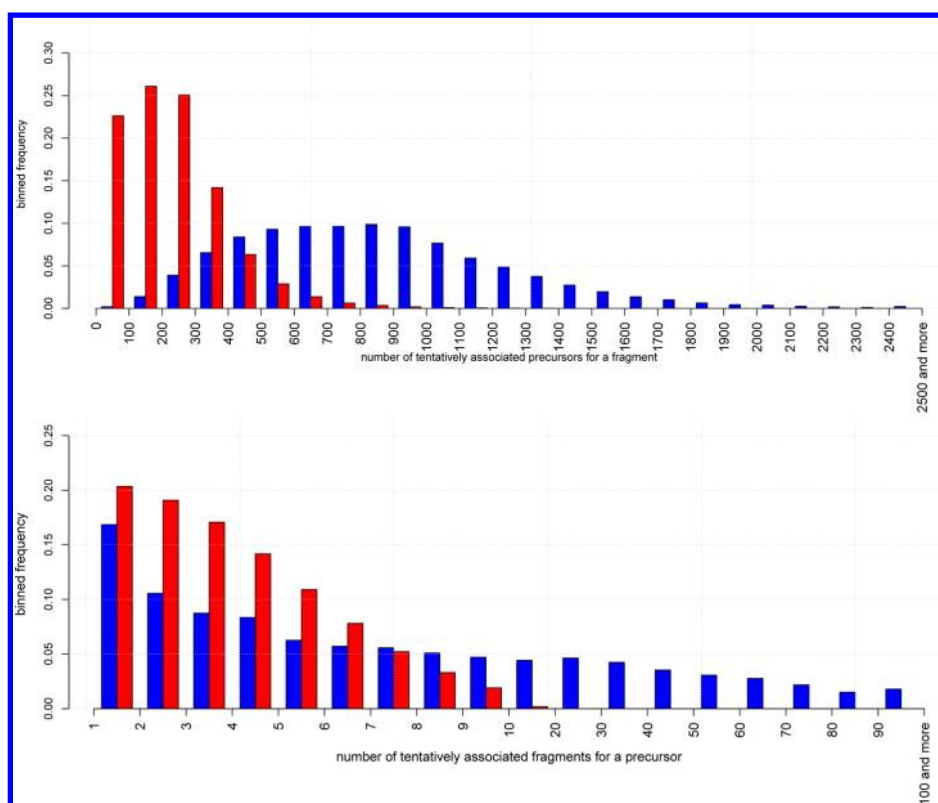
Figure 1. Number of protein identifications for *E. coli* digest standard analysis. (a) Number of protein and peptide identifications uniqure to MS^E (blue) and HDMS^E (red) modes, common in both modes (purple), above saturation threshold in HDMS^E (black; see section Signal Attenuation in HDMSE) at different amounts of digest analyzed. A peptide or protein has only been included if it were identified in 2 out of 3 replicates; the protein FDR has been set to 4%. (b) Number of peptide and protein identifications at different protein FDR for *E. coli* digest standard analysis at 1 μg loading (blue, MSE; red, HDMS^E). Each point is an average of three triplicate acquisitions.

Peptides identified in all three replicates in both modes or a single mode only were selected to investigate the reason for higher number of peptide identifications in HDMS^E. Figure 3a and b gives the scores and the number of fragments that have been assigned to peptides identified in both modes. Peptides identified in both modes have on average higher scores (scores median is 7.8 for MS^E and 8.8 for HDMS^E) and more associated fragments (number of fragments median is 8 for MS^E and 13.3 for HDMS^E) in HDMS^E. Given that fewer fragments are generally associated with precursors in HDMS^E prior to database search, HDMS^E is not only more selective in assigning fragments, but also more accurate, since more of the fragments initially assigned to precursors are subsequently identified as their fragments during the database search. Figure 3c and d gives the scores and the number of associated fragments for peptides identified in a single mode only. As expected, scores are lower than for commonly identified peptides but still higher in HDMS^E than observed in

MS^E (scores median is 6.84 for MS^E and 6.95 for HDMS^E; number of fragments median is 3.7 for MS^E and 6 for HDMS^E). The scores and reliability of peptide identifications could be improved further in HDMS^E in theory, by comparing the predicted IM of a peptide to the experimentally observed for an EMRT.[13,14] A similar calculation is currently performed when the observed retention time of an EMRT is compared to the retention time modeled for a peptide and the magnitude of this correspondence contributes to peptide identification score.[12] However, the prediction of IM for a peptide is not yet implemented in the current version of PLGS (2.5.2); thus, it is likely that the difference in peptide identification scores between modes demonstrated in Figure 3 results solely from a higher number of fragments associated with peptides during database search in HDMS^E.[15-17]

Additional identifications made exclusively in HDMS^E are predominantly from lower intensity ion species (Supplementary Figure 1, Supporting Information), which is consistent with

Figure 2. Blue, MS^E; red, HDMS^E. Binned frequency of the number of (a) fragments tentatively associated with a precursor and (b) precursors tentatively associated with a fragment.

the higher dynamic range of peptide and protein identifications reported previously.[13]

Signal Attenuation in HDMS^E

Comparison of base peak intensity (BPI) traces of *E. coli* digest standard in both modes revealed that HDMS^E appeared less sensitive. BPI traces in HDMS^E were typically approximately one-third as the equivalent MS^E traces (Supplementary Figure 2a, Supporting Information). Inspection of extracted ion chromatograms (XIC) of several of the most intense ions in both modes showed that they are generally less intense and their elution profiles have broader peaks at half height (full width at half maximum, FWHM) in HDMS^E than in MS^E (Supplementary Figure 2b, Supporting Information). This was consistently observed across alternating HDMS^E/MS^E analyses indicating it was independent of the underlying chromatography. To demonstrate this observation systematically we found the ratio of FWHM in HDMS^E and MS^E modes for chromatographic peaks of all ions assigned a peptide identification in three replicates of HDMS^E and MS^E (total of 10593 ions). Ions were binned according to log10 of their intensity in MS^E and their ratio of FWHM between modes plotted (Figure 4). Ions of lower intensities tend to have slightly lower FWHM in HDMS^E, conversely, ions with high intensities have higher FWHM in HDMS^E. The difference in the FWHM of chromatographic profiles between modes is highly statistically significant for all log10 intensity bins (except 4.6 and 4.8 bins in which ions have similar FWHM of elution profiles in MS^E and HDMS^E). Such behavior is consistent with a combination of transmission loss and detector saturation effects, as we demonstrate below.

Figure 5 explains the mechanics of detector saturation by demonstrating what happens in a single mobility experiment comprised of 200 TOF experiments. Without IMS (Figure 5a), ions are recorded continuously (equally distributed between 200 consecutive TOF experiments). Employing IMS (Figure 5b) concentrates ions (the majority of ions are recorded in a small number of TOF experiments, while no ions are observed in other experiments of the IMS cycle). This results in a greater tendency to saturate the detector. The concentration of ions is achieved due to storing the ions in the trapping device prior to evaluating their mobility in the 200 TOF experiments. Trapping is necessary, since no new ions can be allowed into TWIMS, while a cycle of IMS is already in progress. If the IMS peak capacity is increased (Figure 5c), the ions exit IMS in an even tighter package, hence the tendency to saturate the detector becomes even more pronounced. This concentrating effect of TWIMS on a Synapt G2 is dramatic (median FWHM for a mobility profile is 2.9 TOF experiments) and suggests a peptide ion will evoke detector saturation at lower amounts in HDMS^E in contrast to MS^E. A Synapt G2 is equipped with an electron multiplier detector, the output of which is processed by analogue to digital converter (ADC) electronics. The process we refer to as "detector saturation" in this manuscript is strictly speaking detector digitizer saturation. It results from inability of ADC to adequately record the incoming signal from the electron multiplier, rather than from inability of the electron multiplier to produce more signal when more ions arrive at the detector (personal communication with Waters Corp).

To systematically investigate the effect of detector saturation, we selected 2284 *E. coli* peptides that were observed in all three replicates where 1 μg was loaded in both modes. Figure 6 shows the correlation of ion current for common peptides, between replicates of one mode and between modes. The tight intramode correlation between technical replicates is note-
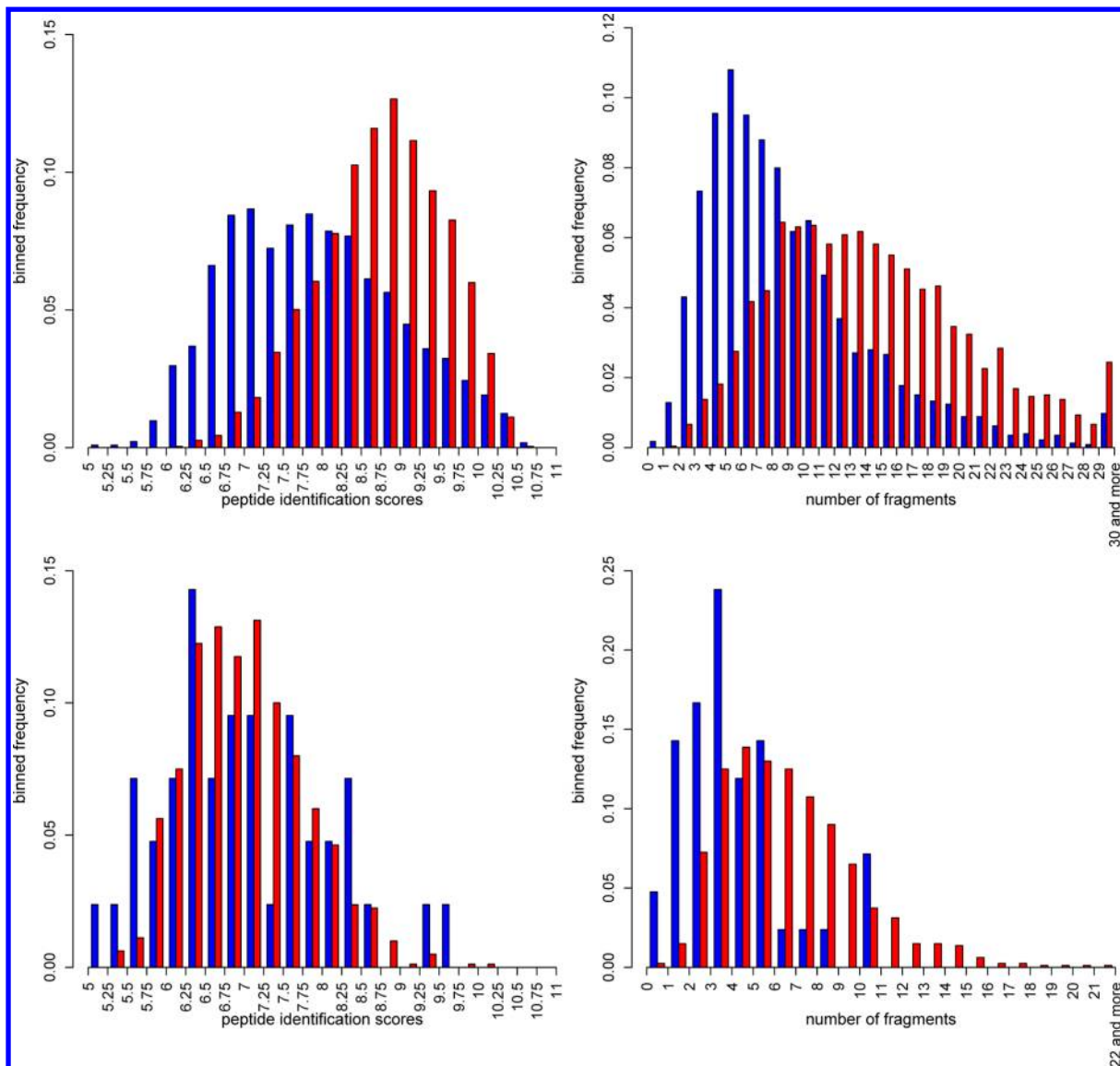
Figure 3. Comparison of peptide identifications between modes (neutral loss fragment ions are not included). Blue, MS^E; red, HDMS^E. (a) Scores for peptides identified in both modes. (b) Number of assigned fragments for peptides identified in both modes. (c) Scores for peptides identified in a single mode only. (d) Number of fragments assigned to peptides identified in a single mode only.

worthy (R^2 0.98 and 0.97 for MS^E and HDMS^E, respectively). The correlation of peptide intensity between different modes is much weaker and appears to have a defined structure (modeled by LOWESS). First, peptides having higher intensity in MS^E tend to lose a higher proportion of their signal in HDMS^E, which results in the LOWESS fit to plateau. This is consistent with detector saturation affecting measurements in HDMS^E. Second, HDMS^E measurements are predominantly lower than their MS^E equivalents across the breadth of the intensity range resulting in the LOWESS fit consistently lying below the 1:1 line and the median ratio of peptide intensity between HDMS^E and MS^E modes being 0.71 To estimate the proportion of peptides which intensity in HDMS^E is higher than saturation threshold we have fitted a linear model through lower intensity measurement which are not expected to saturate. We then used LOWESS to fit a multiple regression model through the data. As expected LOWESS and linear regression models demonstrated almost perfect overlap in the lower intensity range, in the higher intensity range the LOWESS fitted line plateaus

(Figure 6d). We manually selected a point at which LOWESS and linear models no longer overlapped and computed the proportion of peptides which in HDMS^E had higher intensity than that point. We found that 14% of peptides had an intensity higher than the saturation point (80000 counts). A similar analysis for ions and proteins (using the top3 method as implemented in PLGS, where the intensity signal of the three most intense peptides for each protein are summed) (Supplementary Figure 3, Supporting Information) produced an estimate of 14 and 13%, respectively.

If detector saturation was the only HDMS^E effect and it was only intensity related, then peptides of similar intensity in MS^E would be expected to lose the same proportion of their signal in HDMS^E. Our data demonstrate that this is not case as the proportion of intensity lost in HDMS^E with respect to its MS^E intensity is peptide specific. The fact that the degree of signal attenuation is different for peptides of similar intensity in MS^E can be reconciled in two ways.
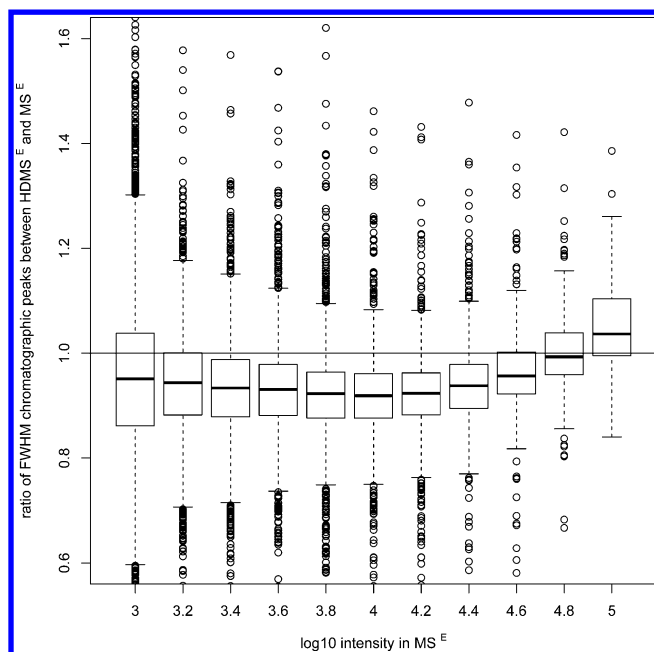
Figure 4. Relationship between the peptide intensity in MS^E and ratio of its FWHM chromatographic peak profiles between modes. Each peptide FWHM has been measured three times in both modes. Each boxplot represents the mean of ratio for all the peptides in the intensity bin.

First, and perhaps counterintuitively, the abundance of a peptide is not necessarily linked directly to its likelihood to saturate the detector, due to the peptide signal being split between multiple isotopes and charge states that result in subpopulations of a peptide ions, each of which arrive at the detector at distinct times in the TOF separation. Moreover, owing to peptide specific chromatographic elution and mobility profiles, the number of TOF experiments that the detector has to record each subpopulation may differ. Together, these peptide-specific features could result in peptides of given intensity evoking detector saturation to different extents.

Second, it is conceivable that a proportion of ions may be lost during the IMS process either during trapping, due to fragmentation of the precursor or due to transmission losses during passage of ions into the high pressure zone in the TWIMS. In either case, an ion will not reach the detector and thus will not be recorded; cumulatively this effect reduces the sensitivity of the analysis. We refer to this scenario as "transmission loss" in the rest of our discussions below.

The effect that IMS has on the FWHM of chromatographic peak for ions (Figure 4) suggests a combination of the two effects. For lower intensity ions, the FWHM is lower since a proportion of the peak is simply not recorded due to transmission loss (Supplementary Figure 4b, Supporting Information). For higher intensity ions the FWHM is higher since all the peak intensity is recorded, but its apex is reduced by detector saturation (Supplementary Figure 4c).

The two explanations of signal loss in HDMS^E (transmission loss and detector saturation only) can also be deconvoluted by performing spike experiments, whereby a group of proteins is analyzed at different loadings. Transmission loss will cause a peptide to lose a constant proportion of its intensity in HDMS^E irrespectively of loading, while detector saturation will cause signal loss at higher loadings only (Figure 7).

Spike Experiments to Investigate Signal Attenuation Nature

To further understand the nature of signal loss in an HDMS^E acquisition, we first performed experiments with the digest of
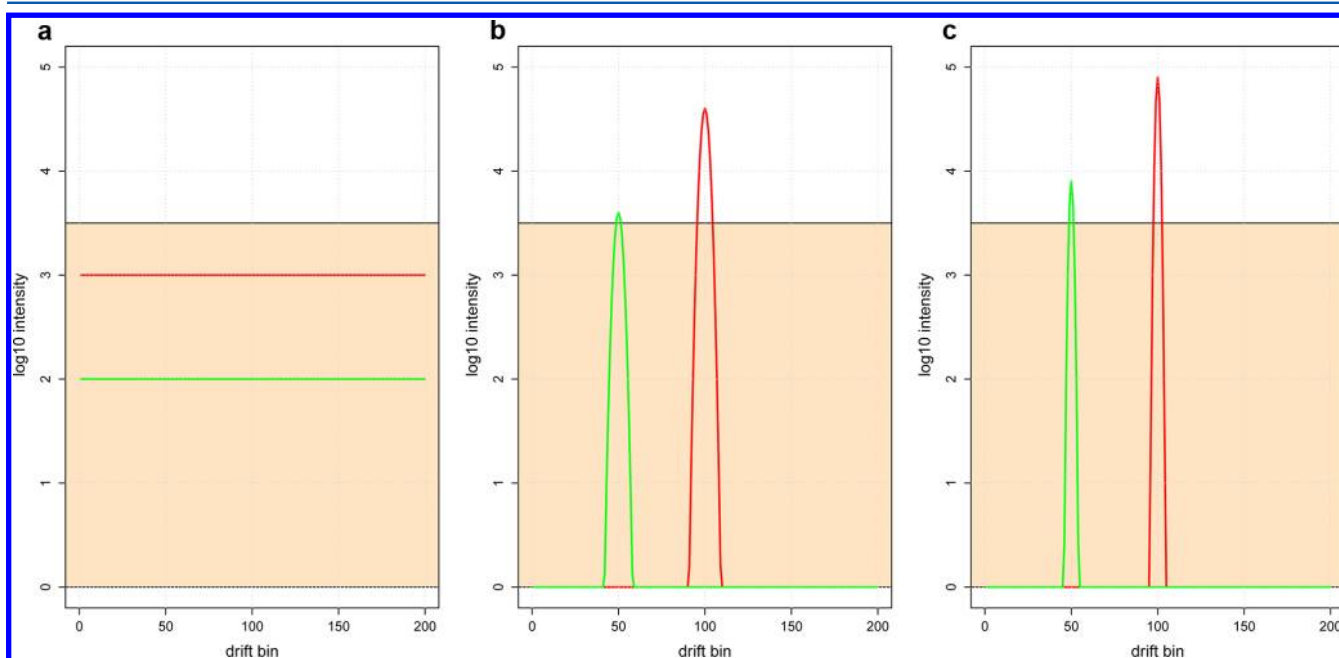

Figure 5. Mechanics of detector saturation in HDMS^E. The plots have been generated such that the intensity (area under the curve) for green and red ions is kept constant. The plots are represented in log scale. The salmon colored area is the linear range of detector, where no saturation is expected. If no IMS is performed, (a) peptide ion intensity is equal across 200 consecutive TOF experiments. If IMS is performed, (b, c) peptide ions are first trapped and then separated by IMS resulting in peptide ions arriving to the detector as a packet, distributed in a small number of TOF experiments. The higher the peak capacity of IMS, the tighter the packets and the more ions exhibit saturation effect (higher peak capacity of IMS in (c) compared to (b) causes green ion to saturate).
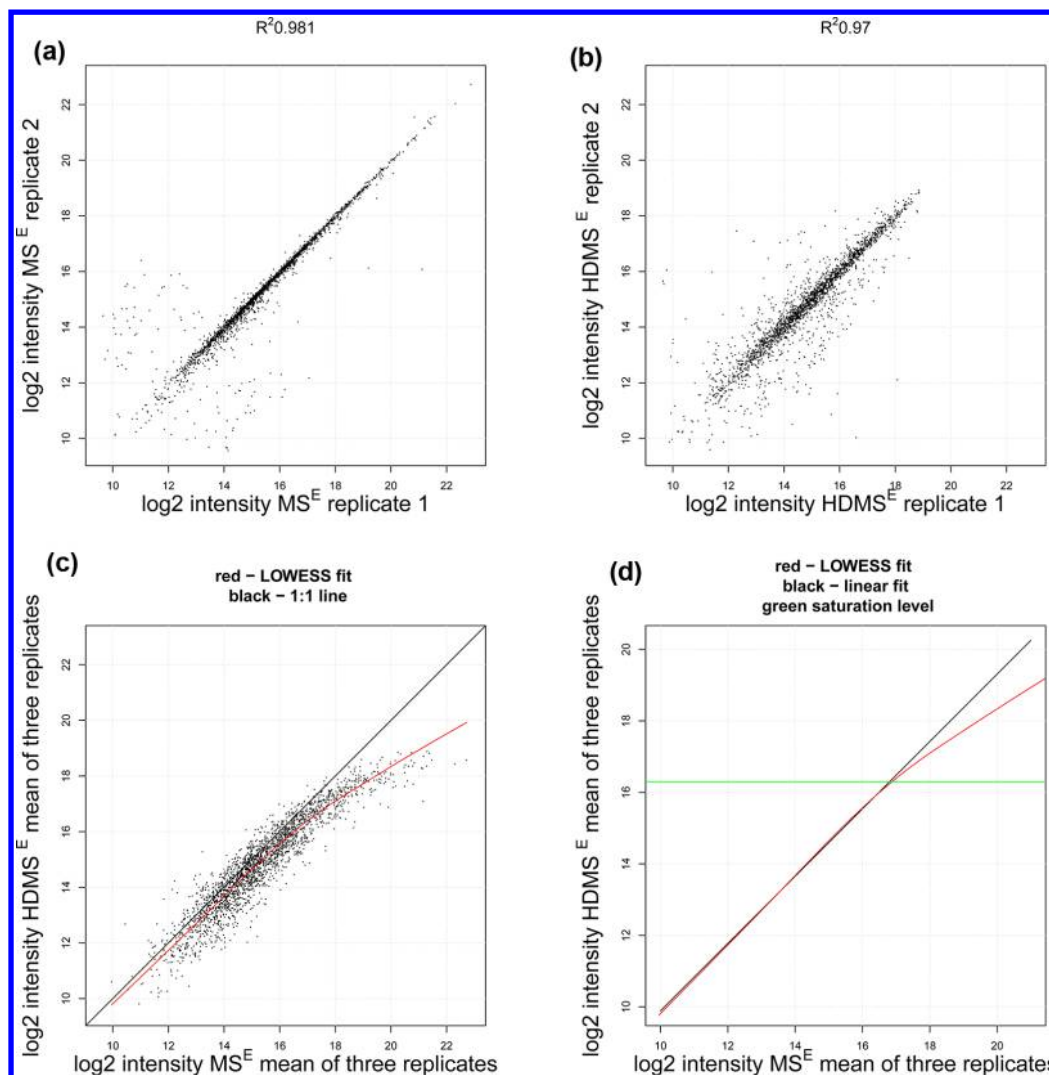
Figure 6. Correlation of peptides' intensities between replicate injections of 1 μg of *E. coli* lysate. (a) MS^E mode: MS^E injection 1 against MS^E injection 2, (b) HDMS^E mode: HDMS^E injection 1 against HDMS^E injection 2, (c) between modes: HDMS^E averaged across three replicates against MS^E averaged across three replicates. Also plotted are 1:1 lines (black) and LOWESS fit (red). (d) Superimposed linear and LOWESS fits through MS^E against HDMS^E data set; the green line denotes saturation threshold.
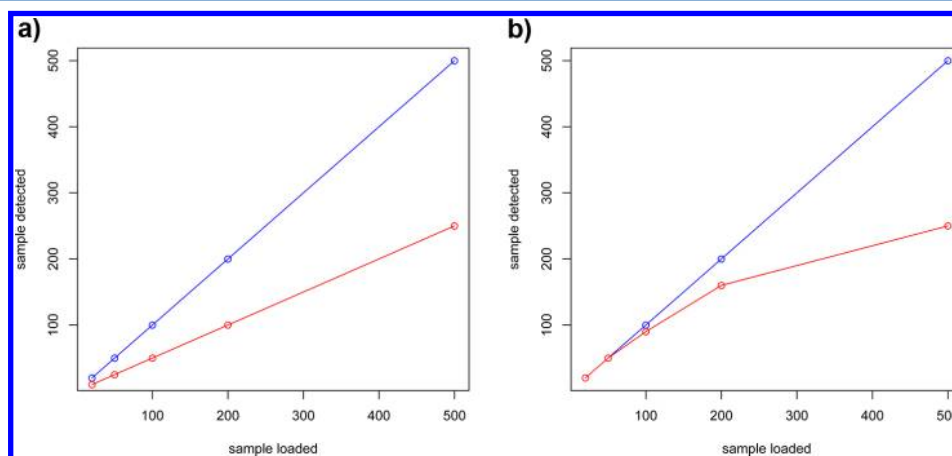
Figure 7. Comparison of detector saturation and transmission loss effects in the spike experiments (data simulated for illustration purposes). Blue line represents recording when neither effect is present; red line demonstrates sensitivity loss due to (a) transmission loss and (b) detector saturation effects.

six equimolar proteins diluted to enable the injection of 20, 50, 100, 200, and 500 fmoles of peptide mixture on column as

described in Table 1. A digest of enolase was invariably added to each injection at 100 fmole loading to allow normalization of
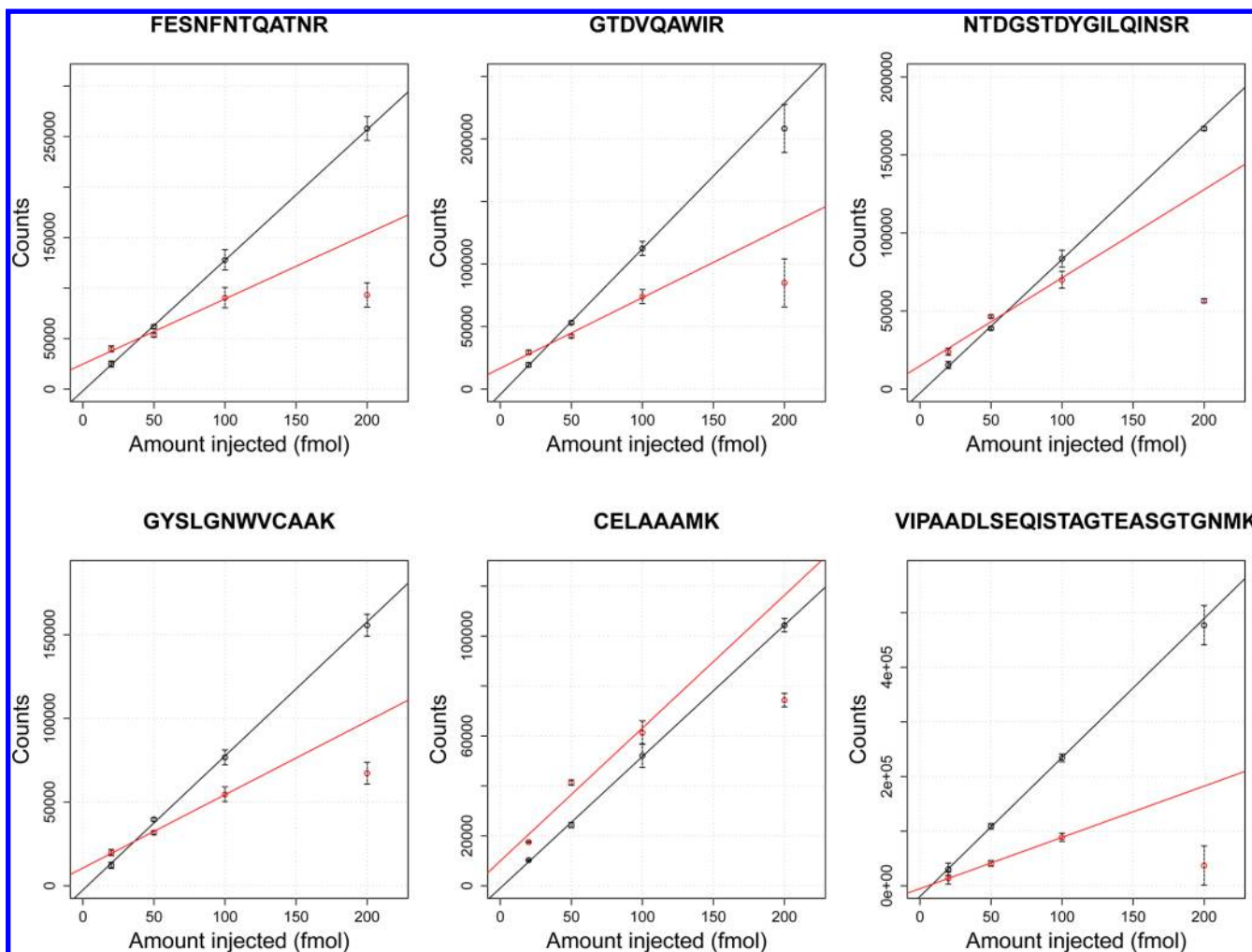
Figure 8. Amount injected on column plotted against the response for six peptides that exhibit saturation behavior in HDMS^E in the six protein mixture experiment. The bars represent standard deviations (black in MS^E, red in HDMS^E).

run to run injection volume variability. The experiment was conducted in triplicate for both modes of analysis, HDMS^E and MS^E. All further analysis was performed on a set of 67 fully tryptic peptides, observed at all loadings in all replicates in both modes. To determine the linearity of the response, peptide intensity was plotted against its loading, a linear regression was extrapolated from the first 3 points (20, 50, 100 fmoles). If the 200 fmole measurement deviated from the value predicted by the regression model by more than 2 standard errors of the mean and at least 20% of the predicted value, the peptide was considered to exhibit a nonlinear response, characteristic of saturation. To demonstrate instances of transmission loss, we calculated the ratio of the slopes of regression lines between the modes. 53 out of 67 peptides demonstrated detector saturation in HDMS^E, and only 1 in MS^E, the median ratio of regression slopes was 0.48. Six instances of detector saturation chosen at random are presented in Figure 8 (a summary of all peptides is presented in Supplementary Figure 5, Supporting Information). Thus, we can conclude that signal loss is a composite of two effects: transmission loss (the ratio of regression slopes is significantly lower than 1) throughout the intensity range, and detector saturation at higher precursor intensities.

To determine whether detector saturation limits the dynamic range of protein quantitation, we used the "top3" method of protein quantitation summing the three most intense peptides

for each protein. This signal was then converted to fmoles by division by the internal standard "top3" signal (100 fmoles of enolase in this study).[11] Figure 9 demonstrates that the amount reported by PLGS was proportional to the amount loaded on column for each of the six proteins in MS^E, but not in HDMS^E. Attenuation of a linear response was observed for loadings of greater than 100 fmoles for all the proteins in HDMS^E.

To establish whether these observations persist in a more complex sample an equivalent experiment was conducted where by a whole cell *E. coli* digest standard was spiked with the six protein digest mixture. One and a half μg of *E. coli* was loaded on column spiked with 25, 50, 75, 100, 250, and 500 fmoles of the six protein mix. The experiment was conducted in triplicate for both modes, a total of 36 injections. Figure 10 demonstrates that the amount reported by PLGS was linearly correlated to the amount of protein loaded on column for all six protein spikes in MS^E. Attenuation of a linear response was observed for all six proteins at both 250 and 500 fmol loading in HDMS^E, analogous to the six protein mixture experiment.

Effects of TWIMS on Peptide Isotopic Envelope

As mentioned above peptide ion properties such as chromatographic elution and IM profiles as well as charge state and isotope intensity distribution are all expected to affect the degree of signal attenuation in HDMS^E. Isotopes of the same
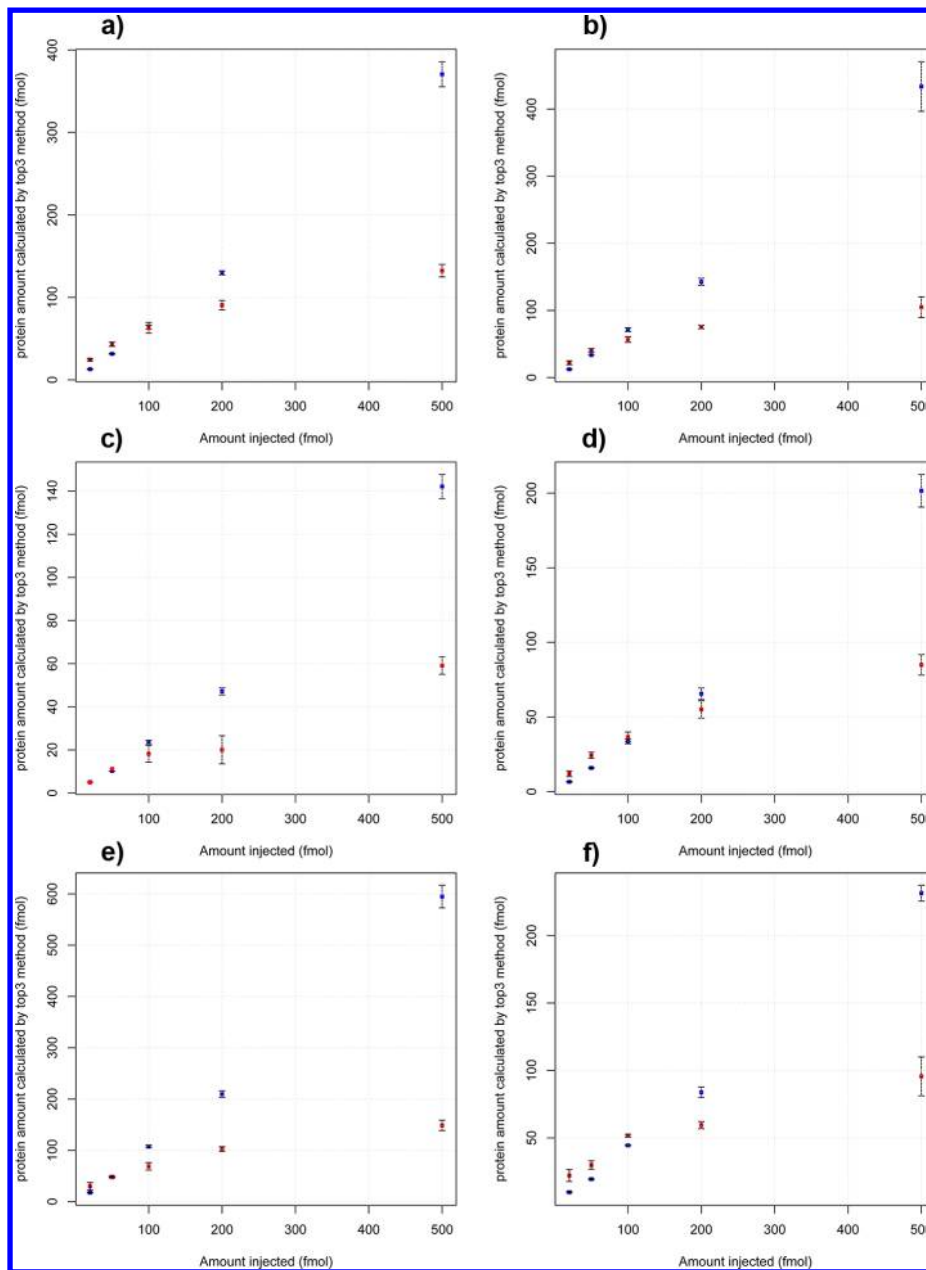
Figure 9. Amount injected on column versus amount reported by PLGS top 3 method (enolase used as calibration protein) for the six protein mixture experiment. (a) Bovine serum albumin, (b) human carbonic anhydrase, (c) bovine beta casein, (d) horse cytochrome C, (e) rabbit glycogen phosphorylase, and (f) chicken lysozyme. Red, measurements made in HDMS^E; blue, measurements made in MS^E. Error bars represent standard deviations.

peptide ion differ only in their m/z ratio and intensity, however, while all other properties remain equal. Isotopes thus enable the deconvolution of transmission loss and detector saturation independently of these peptide specific properties making them perfect models to confirm our interpretations of signal loss in HDMS^E.

Transmission loss and detector saturation are expected to have different effects on the peptide isotopic envelope. While transmission loss is expected to affect all isotopes equally, detector saturation will cause the most intense isotope to lose a higher proportion of its intensity and thus cause a distortion in the isotopic envelope shape (Figure 11).

We employed the ratio of the signal recorded for the first and the second most intense isotopes of a peptide as a numeric representation of isotopic envelope shape and investigated how

this ratio changes between modes (henceforth referred to as "first/second isotope intensity ratio" or ^{12}C/^{13}C for simplicity, even though ^{12}C is not always the most intense isotope). The first/second isotope intensity ratio would be expected to be lower in HDMS^E if detector saturation occurs and is not expected to be affected by transmission loss.

First, we looked into how the first/second isotope ratio changes between modes for peptides from the total *E. coli* digest standard sample (eq 1).

A total of 1257 *E. coli* peptides, which possessed the following properties, were investigated:

(1) at least four recorded consecutive isotopes in all replicates in both modes after the most intense isotope
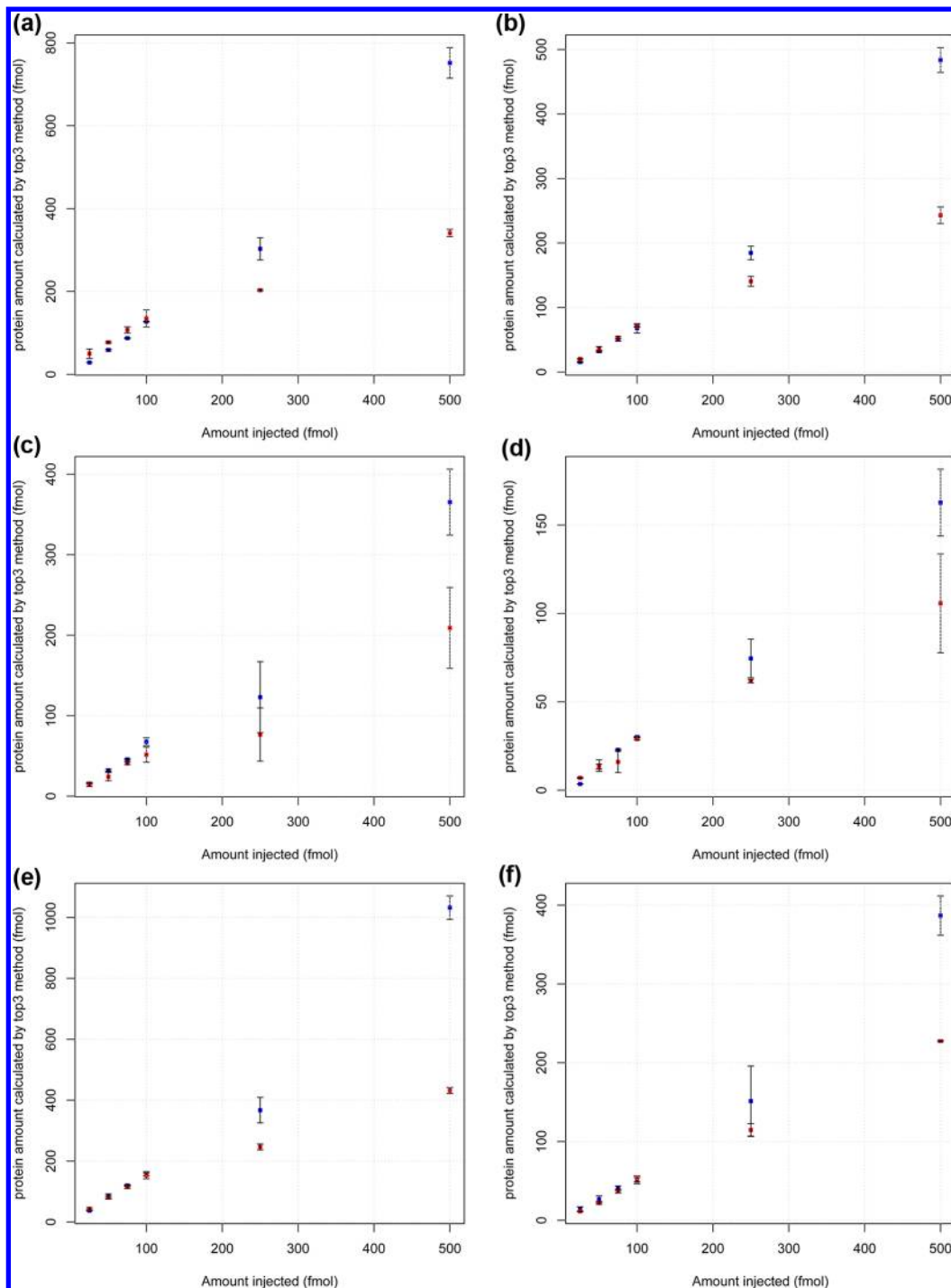
Figure 10. Amount injected on column versus amount reported by PLGS top3 method for the six protein mixture spiked into an *E. coli* lysate experiment. (a) Bovine serum albumin, (b) human carbonic anhydrase, (c) bovine beta casein, (d) horse cytochrome C, (e) rabbit glycogen phosphorylase, and (f) chicken lysozyme. Red, measurements made in HDMS^E; blue, measurements made in MS^E. Error bars represent standard deviations.

(2) 70% or more of their intensity at one of the charge states in both modes

(3) less than 20% CV for all isotopes in both modes.

We arbitrarily chose a first/second isotope ratio 10% lower in HDMS^E than in MS^E (eq 1) to conclude detector saturation at the peptide level.

$$\frac{\text{HDMS}^{E12}\text{C}/^{13}\text{C}}{\text{MS}^{E12}\text{C}/^{13}\text{C}} < 0.9 \qquad (1)$$

Where HDMS^E ^{12}C/^{13}C is the ratio of isotopes in HDMS^E and MS^E ^{12}C/^{13}C is the ratio of isotopes in MS^E. We found that for 21% of all peptides the ratio decreased in HDMS^E by at least 10% indicating that they were subject to detector saturation. Supplementary Figure 6, Supporting Information, shows spectra combined across the chromatographic elution profile for three of such peptides chosen at random to illustrate that isotopic envelope distortion is not an artifact of data processing. Consistent with detector saturation, the majority of the
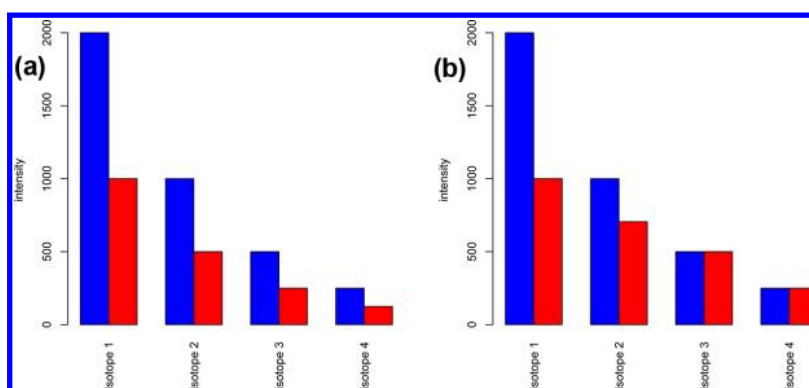
Figure 11. Comparison of detector saturation and transmission loss effects on the peptide isotopic envelope (data simulated for illustration purposes). Blue bars represent the peptide isotopic envelope; red bars demonstrate how the recording changes when (a) transmission loss or (b) detector saturation effects are present.
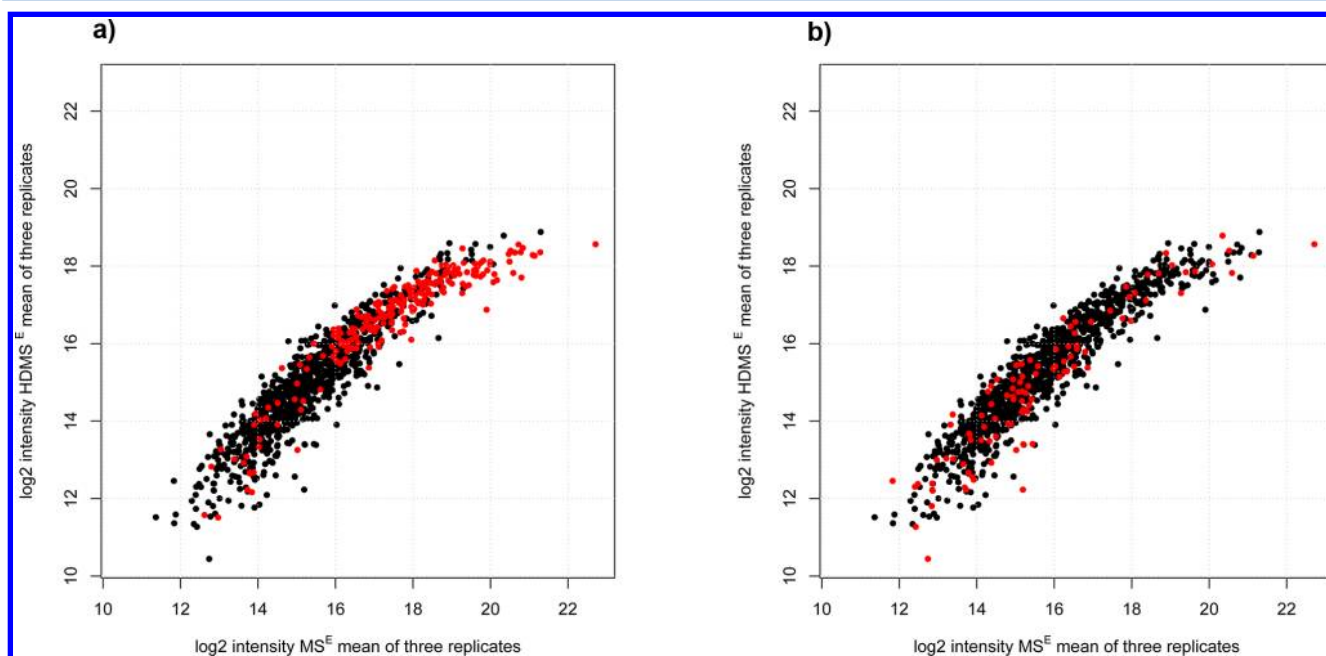
Figure 12. Correlation of peptides' intensities between 1 μg of *E. coli* lysate injections between modes (HDMS^E averaged across three replicates against MS^E averaged across three replicates). (a) In red are peptides that have the first/second isotope ratio decreased in HDMS^E, in black are those that have a similar first/second isotope ratio in both modes. It is noteworthy that peptides which exhibit saturation according to their isotopic envelope distortion (red) are mostly higher intensity peptides in MS^E. (b) In red are peptides that have the penultimate/last isotope ratio decreased in HDMS^E, in black are those that have a similar penultimate/last isotope ratio in both modes. No intensity related bias is apparent.

peptides with distorted isotopic envelope in HDMS^E are at the high intensity end in MS^E (Figure 12a). As expected, no intensity related bias for this ratio was observed when comparing the penultimate/last most intense isotopic ratio between the acquisition modes (Figure 12b).

We next investigated how the first/second isotope ratio changes within each mode upon increasing loading from 20 to 200 fmole using the data from six protein mix experiment. Sixty peptides were chosen that possessed the properties outlined above at 20, 50, 100, and 200 fmole. Forty-four peptides demonstrated a decrease of 10% or more in the isotopic ratio at 200 fmole loading when compared to a 20 fmol loading in HDMS^E (none in MS^E), as in eq 2.

$$\frac{HDMS^E 200 \; fmol \; ^{12}C/^{13}C}{HDMS^E 20 \; fmol \; ^{12}C/^{13}C} < 0.9 \qquad (2)$$

Figure 13 demonstrates that the ratio between the first/second isotope intensity at 20−200 fmol loadings in both modes for 6 such peptides chosen at random (a summary of all peptides is presented in Supplementary Figure 7, Supporting Information). As expected the first/second isotope intensity ratio demonstrates no trend in MS^E, while it decreases in HDMS^E with the increase in loading. Supplementary Figure 8, Supporting Information, shows spectra combined across the chromatographic elution profile for three of such peptides which demonstrate decreased first/second isotope intensity ratio between 20 and 200 fmol loading.

◼ DISCUSSION

The combination of IMS and MS within a single instrument provides an additional dimension of ion separation at no extra cost in instrument time. This exciting synergy of two technologies will undoubtedly have a profound effect on
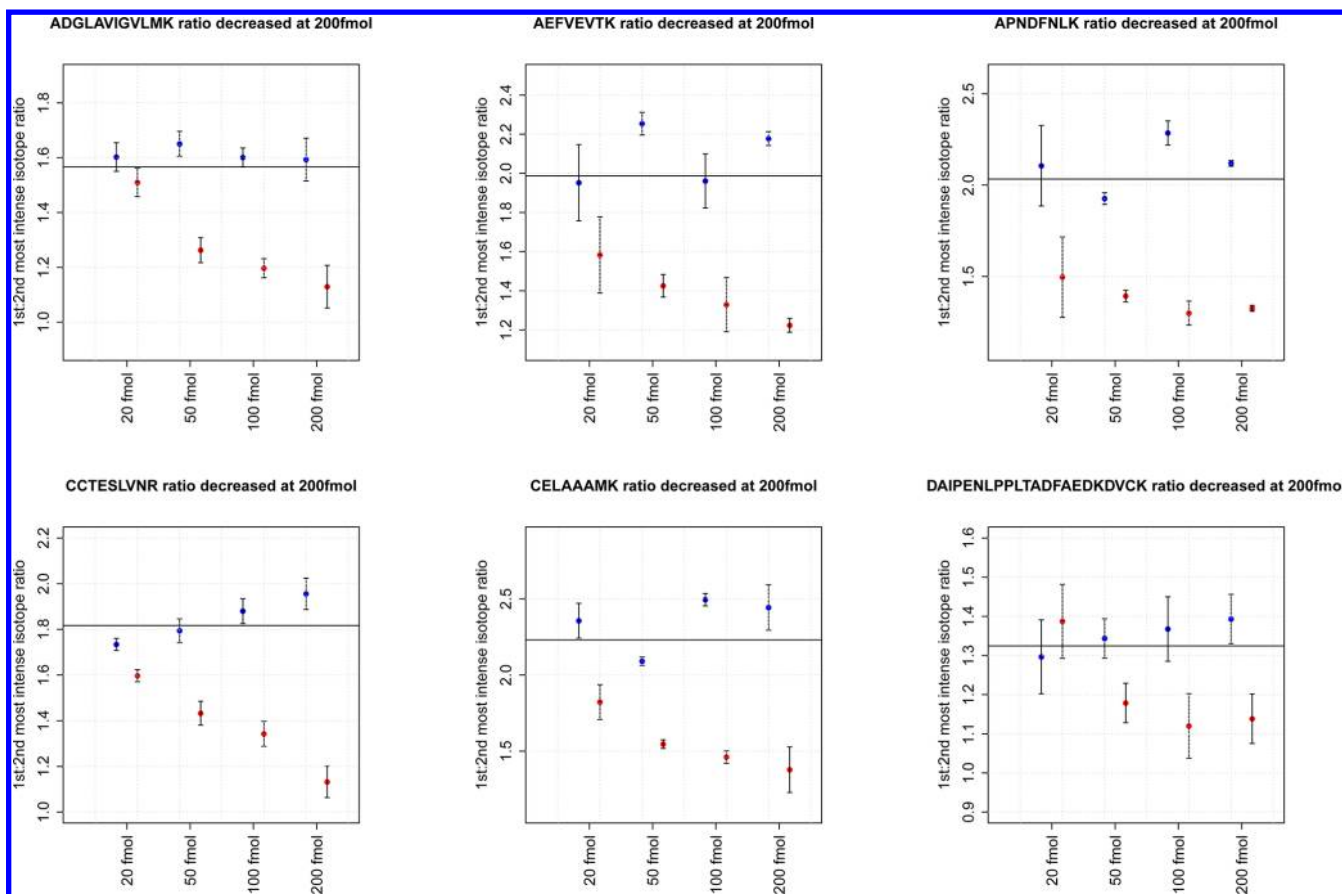
Figure 13. Ratio of the first and second most intense isotopes at different amounts injected for MS^E (blue) and HDMS^E (red) for six peptides that demonstrate saturation; horizontal line indicates theoretical ratio.

proteomics in years to come.[30] However, as with any new technology, IMS/MS requires thorough investigation to better understand its strengths and weaknesses, in order to maximize the benefit of its application.

We chose data-independent acquisition to evaluate the effects of IMS on shotgun proteomics analysis for several reasons. First, all of the fragments and precursors (above the LOD) are recorded and they are sampled throughout their elution profile, at high signal-to-noise ratio, which allows statistically robust comparisons of acquisitions with and without IMS. Second, proteome coverage of data-independent analysis is expected to increase due to better assignment of fragments to precursors.

Indeed, we found that fragments in "high energy" scans can be matched to precursors in "low energy" scans with greater certainty, which is achieved by harnessing the additional discriminatory information captured as precursor drift time. This ultimately results in higher proteome coverage and more confident identifications. Importantly the majority of additionally identified peptides and proteins were found in the lower end of dynamic range. Interestingly the number of identifications from *E. coli* digest increases with loading in HDMS^E, but not MS^E, which demonstrates that increase in sensitivity without increase in specificity does not lead to higher proteome coverage.[34]

Additionally, the application of TWIMS causes a peptide specific decrease in sensitivity (transmission loss) and instrument dynamic range (detector saturation). These effects can be explained by the Synapt G2 instrument design and duty cycle.

Accumulating ions in the trapping device prior to IMS may result in detector saturation. Driving ions into the high pressure TWIMS region may lead to a decrease in sensitivity. In this study we demonstrate the extent of these effects on a Synapt G2 instrument when analyzing simple and complex samples and also use isotopes of the same peptide to further confirm our observations. Arguably, even though the ion losses due to the application of IMS are peptide specific on the Synapt G2 platform, they are nonetheless highly reproducible and do not compromise quantitation precision, as seen by comparing ion intensity within HDMS^E replicates (Figure 6).

The transmission loss introduced by IMS, depends on the instrument's ion path. As discussed previously, quadrupoles and the TOF section of the instrument have to be operated at high vacuum, while IMS performance increases with increasing pressure in IMS zone.[32,35] On instruments with quadrupoles preceding IMS zone (such as the Synapt instrument series), ions have to be moved from low pressure zone (quadrupole) to a high pressure zone (IMS) and then back to a low pressure zone (TOF) again. On instruments where the IMS zone is located near the ion source and is followed by quadrupole and TOF, the ions constantly move from high pressure to lower pressure zones. Moving ions from high pressure zones to low pressure zones (quadrupole and TOF after IMS zone) was initially challenging leading to huge losses in sensitivity (estimated at 99%[36]). The problem was partially solved by Clemmer and colleagues upon the introduction of an orifice-skimmer cone (OSC) at the IMS and quadrupole interface, which improved transmission by a factor of 5−10,[37] which

equates to approximately 5−10% (as estimated by Tang et al.[36]) of ions being successfully transferred from the IMS zone to subsequent segments of the instrument. Recently Smith and colleagues incorporated an ion funnel[38,39] in their IMS/q/TOF instrument that allowed almost lossless transmission between IMS and quadrupole-TOF.[36] As shown in Figure 6, HDMS^E is around 30% less sensitive than MS^E across peptide dynamic range, which we consider to be a function of transmission loss introduced by IMS. This places the Synapt G2 ion transfer efficiency from IMS zone to further segments of the instrument on a scale between IMS-q-TOF platforms equipped with OSC and platforms equipped with ion funnel. Since MS^E and HDMS^E require a number of different adjustable settings (mostly voltage differentials and pressures in TriWave) to transfer ions across the ion path, it is of course possible that utilizing different settings, might cause a lower sensitivity loss, than we estimated. This is however unlikely as the data acquisitions presented in this study were performed with parameters recommended by the manufacturer and similar losses were observed using alternative sets of parameters tested (data not shown).

In our opinion, the primary challenge of label-free quantitation on the q-TWIMS-TOF Synapt G2 design is the reduction of signal linearity in the upper end of dynamic range. It is noteworthy that Clemmer and co-workers reported detector saturation on a platform with a different type of IMS (drift tube rather than TWIMS) and a different trap (linear octopole trap),[23] but also suggesting that the detector saturation effect results from an ion concentration effect (see Figure 5). We have demonstrated the detector saturation effect on two extremes of proteomics analysis: a low complexity mixture analyzed by a steep LC-gradient with highly abundant constituents (6 protein spike experiment) and a high complexity mixture (*E. coli* digest standard) analyzed using a longer gradient. While detector saturation has a dramatic effect on the former experiment its effect appears to be more subtle for the latter. Several simple and easy to implement solutions can be suggested to address the problem.

First and most obvious solution is to only use workflows, where detector saturation is not a problem. To develop such workflows a researcher must consider a number of issues, including the peak capacity of IMS and LC (the higher the peak capacity of these separations, the higher the ion current for a peptide at its apex and thus its tendency to saturate the detector). Moreover, if additional prefractionation or enrichment is performed at the peptide or protein level, less sample should be analyzed during LC−MS, since prefractionation or enrichment cause a proportional increase of some components in a mixture (for example it is usual to analyze more sample in 2D-LC than in 1D-LC because of lower amounts of sample utilized in 1D-LC, which will contribute to detector saturation problem). Finally, the actual focus of the research is important, that is, whether researcher is interested in higher abundance proteins for example, when studying metabolic enzymes or lower abundance proteins when studying biomarkers of diseases in plasma. In the latter cases detector saturation in HDMS^E might not be problematic at all, as the IMS peak capacity will increase quantitation accuracy of lower abundance proteins and increase probability of their identification.[24] Also it might seem counterintuitive that the proportion of proteins and peptides over the saturation threshold is similar, since some sort of averaging effect on protein level might be assumed. However, the protein quantitation reported in this study was performed by top3 method, where the more intense peptides are weighted more highly than less intense peptides in calculation to determine protein amount. A relative quantitation method where all peptides are given equal contribution might be less prone to accuracy bias, but at the same time will suffer in precision since higher intense peptides are recorded more precisely.

A second set of solutions are purely instrumental, for example increasing dynamic range of ion detection system. This is by no means a trivial task (see Chernushevich et al.[40] for a review on TOF detector systems). Furthermore, since even the simplest proteome components span at least 5−6 orders of magnitude[41] and current detectors achieve 4 orders of linearity at best we are far from covering the entire proteome dynamic range as it is without further adding to the problem. A second solution is to combine precursor acquisitions with and without ion mobility in a single analysis, hence there will be three functions in the acquisition: "low energy without IMS", "low energy with IMS" and "high energy with IMS" (fragmentation post IMS). In this setup "low energy with IMS" and "high energy with IMS" functions would be used to assign fragments to precursors and for subsequent identification and "low energy without IMS" would be used for quantitation. However, since IMS adds peak capacity to separation, removing IMS from the quantitation may have an adverse effect on accuracy and precision of MS1 quantitation, especially on lower abundance peptides.

Finally, bioinformatics solutions could be suggested to address the problem. For example, similarly to combining acquisitions with and without IMS in a single run as described above it is possible to analyze the sample with and without IMS and identify peptides in HDMS^E. It would then be possible to determine the EMRTs in MS^E data corresponding to HDMS^E identifications based on the similarity of their retention time and measured mass. This should not cause a significant increase in instrument time since a sample needs to be run in MS^E a number of times for accurate quantitation and only once in HDMS^E for peptide identification. The application of this method is demonstrated in ref 42 describing the Synapter software we have developed for this purpose. A very different approach is to quantify only on isotopes below the saturation threshold, on fragments or to try and predict the actual intensity of a saturated peptide based on its isotopic envelope. This task is not new and methods of such postacquisition corrections have been suggested for acquisitions performed on instruments with TDC detectors and shown to restore at least an order of magnitude of detector linearity. Our data on peptide isotope envelope distortion suggests such a possibility; however, methods developed for TDC detector saturation correction are not directly applicable for correction of ADC detector saturation and will require additional advancement.

■ ASSOCIATED CONTENT

Ⓢ Supporting Information

Supplemental figures. This material is available free of charge via the Internet at http://pubs.acs.org.

■ AUTHOR INFORMATION

Corresponding Author

*E-mail: k.s.lilley@bioc.cam.ac.uk. Tel: +441223760255. Fax: +441223760241.

■ **REFERENCES**

(1) Schulze, W. X.; Usadel, B. Quantitation in mass-spectrometry-based proteomics. *Annu. Rev. Plant Biol.* **2010**, *61*, 491−516.

(2) Sadygov, R. G.; Cociorva, D.; Yates, J. R., 3rd Large-scale database searching using tandem mass spectra: looking up the answer in the back of the book. *Nat. Methods* **2004**, *1*, 195−202.

(3) Ong, S.-E.; Kratchmarova, I.; Mann, M. Properties of 13C-substituted arginine in stable isotope labeling by amino acids in cell culture (SILAC). *J. Proteome Res.* **2003**, *2*, 173−181.

(4) Thompson, A.; Schäfer, J.; Kuhn, K.; Kienle, S.; Schwarz, J.; Schmidt, G.; Neumann, T.; Johnstone, R.; Mohammed, A. K. A.; Hamon, C. Tandem mass tags: a novel quantification strategy for comparative analysis of complex protein mixtures by MS/MS. *Anal. Chem.* **2003**, *75*, 1895−1904.

(5) Neilson, K. A.; Ali, N. A.; Muralidharan, S.; Mirzaei, M.; Mariani, M.; Assadourian, G.; Lee, A.; van Sluyter, S. C.; Haynes, P. A. Less label, more free: approaches in label-free quantitative mass spectrometry. *Proteomics* **2011**, *11*, 535−553.

(6) Ishihama, Y.; Oda, Y.; Tabata, T.; Sato, T.; Nagasu, T.; Rappsilber, J.; Mann, M. Exponentially modified protein abundance index (emPAI) for estimation of absolute protein amount in proteomics by the number of sequenced peptides per protein. *Mol. Cell. Proteomics* **2005**, *4*, 1265−1272.

(7) Geromanos, S. J.; Vissers, J. P. C.; Silva, J. C.; Dorschel, C. A.; Li, G.-Z.; Gorenstein, M. V.; Bateman, R. H.; Langridge, J. I. The detection, correlation, and comparison of peptide precursor and product ions from data independent LC-MS with data dependant LC-MS/MS. *Proteomics* **2009**, *9*, 1683−1695.

(8) Gillet, L. C.; Navarro, P.; Tate, S.; Roest, H.; Selevsek, N.; Reiter, L.; Bonner, R.; Aebersold, R. Targeted data extraction of the MS/MS spectra generated by data independent acquisition: a new concept for consistent and accurate proteome analysis. *Mol. Cell. Proteomics* **2012**, *11* (6), No. O111.016717.

(9) Levin, Y.; Hradetzky, E.; Bahn, S. Quantification of proteins using data-independent analysis (MSE) in simple andcomplex samples: a systematic evaluation. *Proteomics* **2011**, *11*, 3273−3287.

(10) Silva, J. C.; Denny, R.; Dorschel, C. A.; Gorenstein, M.; Kass, I. J.; Li, G.-Z.; McKenna, T.; Nold, M. J.; Richardson, K.; Young, P.; Geromanos, S. Quantitative proteomic analysis by accurate mass retention time pairs. *Anal. Chem.* **2005**, *77*, 2187−2200.

(11) Silva, J. C.; Gorenstein, M. V.; Li, G.-Z.; Vissers, J. P. C.; Geromanos, S. J. Absolute quantification of proteins by LCMSE: a virtue of parallel MS acquisition. *Mol. Cell. Proteomics* **2006**, *5*, 144−156.

(12) Li, G.-Z.; Vissers, J. P. C.; Silva, J. C.; Golick, D.; Gorenstein, M. V.; Geromanos, S. J. Database searching and accounting of multiplexed precursor and product ion spectra from the data independent analysis of simple and complex peptide mixtures. *Proteomics* **2009**, *9*, 1696−1719.

(13) Valentine, S. J.; Ewing, M. A.; Dilger, J. M.; Glover, M. S.; Geromanos, S.; Hughes, C.; Clemmer, D. E. Using Ion Mobility Data to Improve Peptide Identification: Intrinsic Amino Acid Size Parameters. *J. Proteome Res.* **2011**, *10*, 2318−2329.

(14) Shah, A. R.; Agarwal, K.; Baker, E. S.; Singhal, M.; Mayampurath, A. M.; Ibrahim, Y. M.; Kangas, L. J.; Monroe, M. E.; Zhao, R.; Belov, M. E.; Anderson, G. A.; Smith, R. D. Machine learning based prediction for peptide drift times in ion mobility spectrometry. *Bioinformatics* **2010**, *26*, 1601−1607.

(15) Chamrad, D.; Meyer, H. E. Valid data from large-scale proteomics studies. *Nat. Methods* **2005**, *2*, 647−648.

(16) Miyamoto, M.; Yoshida, Y.; Taguchi, I.; Nagasaka, Y.; Tasaki, M.; Zhang, Y.; Xu, B.; Nameta, M.; Sezaki, H.; Cuellar, L. M.; Osawa, T.; Morishita, H.; Sekiyama, S.; Yaoita, E.; Kimura, K.; Yamamoto, T. In-depth proteomic profiling of the normal human kidney glomerulus using two-dimensional protein prefractionation in combination with liquid chromatography-tandem mass spectrometry. *J. Proteome Res.* **2007**, *6*, 3680−3690.

(17) Michalski, A.; Cox, J.; Mann, M. More than 100,000 detectable peptide species elute in single shotgun proteomics runs but the majority is inaccessible to data-dependent LC−MS/MS. *J. Proteome Res.* **2011**, *10*, 1785−1793.

(18) Kennedy, J.; Yi, E. C. Use of gas-phase fractionation to increase protein identifications: application to the peroxisome. *Methods Mol. Biol.* **2008**, *432*, 217−228.

(19) Masselon, C.; Anderson, G. A.; Harkewicz, R.; Bruce, J. E.; Pasa-Tolic, L.; Smith, R. D. Accurate mass multiplexed tandem mass spectrometry for high-throughput polypeptide identification from mixtures. *Anal. Chem.* **2000**, *72*, 1918−1924.

(20) Panchaud, A.; Scherl, A.; Shaffer, S. A.; von Haller, P. D.; Kulasekara, H. D.; Miller, S. I.; Goodlett, D. R. Precursor acquisition independent from ion count: how to dive deeper into the proteomics ocean. *Anal. Chem.* **2009**, *81*, 6481−6488.

(21) Venable, J. D.; Dong, M.-Q.; Wohlschlegel, J.; Dillin, A.; Yates, J. R. Automated approach for quantitative analysis of complex peptide mixtures from tandem mass spectra. *Nat. Methods* **2004**, *1*, 39−45.

(22) Geiger, T.; Cox, J.; Mann, M. Proteomics on an Orbitrap benchtop mass spectrometer using all-ion fragmentation. *Mol. Cell. Proteomics* **2010**, *9*, 2252−2261.

(23) Myung, S.; Lee, Y. J.; Moon, M. H.; Taraszka, J.; Sowell, R.; Koeniger, S.; Hilderbrand, A. E.; Valentine, S. J.; Cherbas, L.; Cherbas, P.; Kaufmann, T. C.; Miller, D. F.; Mechref, Y.; Novotny, M. V.; Ewing, M. A.; Sporleder, C. R.; Clemmer, D. E. Development of high-sensitivity ion trap ion mobility spectrometry time-of-flight techniques: a high-throughput nano-LC-IMS-TOF separation of peptides arising from a Drosophila protein extract. *Anal. Chem.* **2003**, *75*, 5137−5145.

(24) Valentine, S. J.; Plasencia, M. D.; Liu, X.; Krishnan, M.; Naylor, S.; Udseth, H. R.; Smith, R. D.; Clemmer, D. E. Toward Plasma Proteome Profiling with Ion Mobility-Mass Spectrometry. *J. Proteome Res.* **2006**, *5*, 2977−2984.

(25) Taraszka, J. A.; Kurulugama, R.; Sowell, R. A.; Valentine, S. J.; Koeniger, S. L.; Arnold, R. J.; Miller, D. F.; Kaufman, T. C.; Clemmer, D. E. Mapping the proteome of Drosophila melanogaster: analysis of embryos and adult heads by LC-IMS-MS methods. *J. Proteome Res.* **2005**, *4*, 1223−1237.

(26) Hoaglund-Hyzer, C. S.; Li, J.; Clemmer, D. E. Mobility labeling for parallel CID of ion mixtures. *Anal. Chem.* **2000**, *72*, 2737−2740.

(27) Baker, E. S.; Livesay, E. A.; Orton, D. J.; Moore, R. J.; Danielson, W. F., 3rd; Prior, D. C.; Ibrahim, Y. M.; LaMarche, B. L.; Mayampurath, A. M.; Schepmoes, A. A.; Hopkins, D. F.; Tang, K.; Smith, R. D.; Belov, M. E. An LC-IMS-MS platform providing increased dynamic range for high-throughput proteomic studies. *J. Proteome Res.* **2010**, *9*, 997−1006.

(28) Geromanos, S. J.; Hughes, C.; Ciavarini, S.; Vissers, J. P. C.; Langridge, J. I. Using ion purity scores for enhancing quantitative accuracy and precision in complex proteomics samples. *Anal. Bioanal. Chem.* **2012**, *404* (4), 1127−1139.

(29) Valentine, S. J.; Counterman, A. E.; Hoaglund, C. S.; Reilly, J. P.; Clemmer, D. E. Gas-phase separations of protease digests. *J. Am. Soc. Mass Spectrom.* **1998**, *9*, 1213−1216.

(30) Bohrer, B. C.; Merenbloom, S. I.; Koeniger, S. L.; Hilderbrand, A. E.; Clemmer, D. E. Biomolecule analysis by ion mobility spectrometry. *Annu. Rev. Anal. Chem.* **2008**, *1*, 293−327.

(31) Hoaglund, C. S.; Valentine, S. J.; Clemmer, D. E. An Ion Trap Interface for ESI−Ion Mobility Experiments. *Anal. Chem.* **1997**, *69*, 4156−4161.

(32) Davis, E. J.; Grows, K. F.; Siems, W. F.; Hill, H. H., Jr Improved ion mobility resolving power with increased buffer gas pressure. *Anal. Chem.* **2012**, *84*, 4858−4865.

(33) Moore, S.; Spackman, D. H.; Stein, W. H. Automatic recording apparatus for use in the chromatography of amino acids. *Fed. Proc.* **1958**, *17*, 1107−1115.

(34) Geromanos, S. J.; Hughes, C.; Golick, D.; Ciavarini, S.; Gorenstein, M. V.; Richardson, K.; Hoyes, J. B.; Vissers, J. P. C.; Langridge, J. I. Simulating and validating proteomics data and search results. *Proteomics* **2011**, *11*, 1189−1211.

(35) Davis, E. J.; Dwivedi, P.; Tam, M.; Siems, W. F.; Hill, H. H. High-pressure ion mobility spectrometry. *Anal. Chem.* **2009**, *81*, 3270−3275.

(36) Tang, K.; Shvartsburg, A. A.; Lee, H.-N.; Prior, D. C.; Buschbach, M. A.; Li, F.; Tolmachev, A.; Anderson, G. A.; Smith, R. D. High-Sensitivity Ion Mobility Spectrometry/Mass Spectrometry Using Electrodynamic Ion Funnel Interfaces. *Anal. Chem.* **2005**, *77*, 3330−3339.

(37) Lee, Y. J.; Hoaglund-Hyzer, C. S.; Taraszka, J. A.; Zientara, G. A.; Counterman, A. E.; Clemmer, D. E. Collision-induced dissociation of mobility-separated ions using an orifice-skimmer cone at the back of a drift tube. *Anal. Chem.* **2001**, *73*, 3549−3555.

(38) Shaffer, S. A.; Tang, K.; Anderson, G. A.; Prior, D. C.; Udseth, H. R.; Smith, R. D. A novel ion funnel for focusing ions at elevated pressure using electrospray ionization mass spectrometry. *Rapid Commun. Mass Spectrom.* **1997**, *11*, 1813−1817.

(39) Kelly, R. T.; Tolmachev, A. V.; Page, J. S.; Tang, K.; Smith, R. D. The ion funnel: theory, implementations, and applications. *Mass Spectrom. Rev.* **2010**, *29*, 294−312.

(40) Chernushevich, I. V.; Loboda, A. V.; Thomson, B. A. An introduction to quadrupole-time-of-flight mass spectrometry. *J. Mass Spectrom.* **2001**, *36*, 849−865.

(41) Ghaemmaghami, S.; Huh, W.-K.; Bower, K.; Howson, R. W.; Belle, A.; Dephoure, N.; O'Shea, E. K.; Weissman, J. S. Global analysis of protein expression in yeast. *Nature* **2003**, *425*, 737−741.

(42) Bond, N. J.; Shliaha, P. V.; Lilley, K. S.; Gatto, L. Improving qualitative and quantitative performance for MS^E-based label-free proteomics. *J. Proteome Res.* **2013**, DOI: 10.1021/pr300776k.